Predicting Sediment Discharge at Water Treatment Plant Under Different Land Use Scenarios Coupling Expert-Based GIS Model and Deep Neural Network

Edouard Patault[1], Valentin Landemaine[2], Jérôme Ledun[3], Arnaud Soulignac[4], Matthieu Fournier[1], Jean-
François Ouvry[3], Olivier Cerdan[2], Benoit Laignel[1]

[1]Normandie UNIV, UNIROUEN, UNICAEN, CNRS, M2C, FED-SCALE, Rouen, France
[2]BRGM, 3 avenue Claude Guillemin, BP6009, F-45060 Orléans Cedex 2, France
[3]AREAS, 2 avenue Foch, F-76460 Saint-Valéry-en-Caux, France
[4]BRGM, 1039 rue de Pinville, F-34000 Montpellier, France

Correspondence to: Edouard Patault (edouard.patault1@univ-rouen.fr)

Abstract. ~~Excessive sediment discharge at karstic springs and thus, water treatment plants, can be highly disruptive~~. It is essential for catchment stakeholders and drinking water supplier to ~~reduce~~ the impact of sediment on potable water supply, but their strategic choices must be based on simulations, integrating surface and groundwater transfers, and taking into account possible changes in land use. Karstic environments are particularly challenging as they face a lack of accurate physical description for the modelling process, and they can be ~~seen as a black-box~~ due to the non-linearity of the processes generating sediment discharge. The aim of the study was to assess the sediment discharge variability at a water treatment plant according to multiple realistic land use scenarios. To reach that goal, we developed a new coupled modelling approach with an erosion-runoff GIS model (WaterSed) and a deep neural network. The model was used in the Radicatel catchment (106 km² in Normandy, France) where karstic spring water is extracted to a water treatment plant. The sediment discharge was simulated for five designed storm projects under current land use and compared to three land use scenarios (baseline, ploughing up of grassland, eco-engineering, best farming practices). Daily rainfall time series and WaterSed modelling outputs extracted at connected sinkholes were used as input data for the deep neural network model. The model structure was found by a classical trial and error procedure, and the model was trained on two significant hydrologic years. Evaluation on a test set showed a good performance of the model (NSE = 0.82), and the application of a monthly backward chaining nested cross validation revealed that the model is able to generalize on new datasets. Simulations made for the three land use scenarios suggested that ploughing up 33 % of grasslands would not increase significantly sediment discharge at the water treatment plant (5 % ~~in~~ average). ~~In the opposite~~, eco-engineering and best farming practices will significantly reduce sediment discharge at the water treatment plant (respectively in the range of 10-44 and 24-61 %). The coupling of these two strategies is the most efficient since it affects the hydro-sedimentary production and transfer processes (decreasing sediment discharge from 40 to 80 %). The coupled modelling approach developed in this study offers interesting opportunities for sediment discharge prediction at karstic springs or water treatment plant under multiple land use scenarios. It also provides robust decision-making tools for land use planning and drinking water suppliers.

Key words: erosion; runoff; karst; deep neural network; WaterSed model; land use scenarios

1 Introduction

35 In karstic environment, erosion and runoff ~~on catchment~~ can lead to ~~excessive transfer of~~ sediments in ~~raw water~~. Sediment discharge (SD) can occur through rapid and direct transfer via sinkholes, and/or via re-suspension of sediment in karst network (Masséi et al., 2003). For ~~drinking water supplier~~, excessive sediment input can be highly disruptive requiring additional ~~water~~ treatment, or in the worst cases, temporary shutdown of ~~a~~ Water Treatment Plant (WTP; Stevenson et al., 2019). Impacts can be significant including restrictions on the use of drinking water ~~for individuals~~. Upper-Normandy (France) is particularly

40 affected, and the economic cost linked to the restrictions on the use of drinking water was estimated to €5 million between 1992 and 2018 (Patault et al., 2019). 10000 to 20000 people are still affected every year by restrictions on the use of drinking water in ~~this~~ region (ARS, 2013). Reducing sediment delivery to sinkholes ~~located on water catchment~~ is therefore essential for catchment managers in order to reduce the impact on potable water supply. One way is to build complex modelling chain, integrating surface and groundwater transfers ~~for the decision-making process~~. Several approaches have been proposed to

45 model erosion/runoff ~~on catchment~~ and karstic response induced by rainfall, but these approaches are often treated separately. Many studies in the literature have focused on hillslopes erosion processes using different types of erosion models ~~developed through the past years~~ (Merritt et al., 2003; de Vente et al., 2013). Empirical models, such as RUSLE (Renard, 1994), are frequently used because of limited data requirement but are not able to fully represent spatial and temporal dynamic of erosion processes at the catchment scale. Physical models, such as WEPP or LISEM (Laflen et al., 1991; Takken et al., 1999), can

50 more accurately describe processes but may require many input parameters that are not available for application on large areas. Expert-based models (e.g. STREAM, WaterSed (Cerdan et al., 2001; Landemaine, 2016) offers an interesting compromise focusing on the main driving factors of runoff and erosion. These models have been ~~especially~~ designed on cultivated areas of the European loess belt and are particularly efficient where hortonian overland flow dominates (Souchère et al., 2005; Evrard et al., 2010; Landemaine, 2016). However, despite the fact that some of ~~these~~ hillslopes erosion studies are conducted in similar

55 karstic environment, they do not account for the transmissivity loss of water and sediment in sinkholes. ~~On the other hand,~~ studies have focused on modelling karst processes, mainly karstic floods but ~~few on~~ sedimentary fluxes (see review of Hartmann et al., 2014). Due to the non-linearity of the processes generating sediment at karstic springs, and the lack of accurate physical description of karstic environments, modelling surface-subsurface interactions with physical models can ~~be~~ therefore a difficult task (Savary et al., 2017; Jourde et al., 2018). Based on systemic approach, as initiated by Mangin (1984), the karst

60 can be considered as a system able to both transform an input (rainfall) into an output (discharge) and evaluate the input-output relation using mathematical functions. This approach ~~refers to~~ 'black-box' models and recent research emphasized the use of data-driven techniques for 'black-box' models, such as Deep Neural Network (DNN). DNN ~~consists of~~ advanced Artificial Neural Networks (ANN) which ~~had gained~~ momentum since 2012 in computing sciences, and ~~for which the~~ adoption has been gradual in hydrology (Shen, 2018). DNN are now commonly used for modelling real world problems due to their ability to

65 ~~model~~ and generalize complex non-linear relationships between inputs and outputs (Meyers et al., 2016; 2017; Hafeez et al., 2019). As stated by Shen (2018), DNN have now surpassed traditional statistical methods. Limited but conclusive applications were made to predict inflow to ~~dams~~, water level of combined sewage outflow structure, turbidity, ~~karst~~ flood forecasting, and ~~integration~~ in rainfall-runoff modelling to predict streamflow ~~in basins~~ (Siou et al., 2011; Bai et al., 2016; Savary et al., 2017; Hu et al., 2018; Kratzert et al., 2018). DNN can help provide both stronger predictive capabilities and a complementary avenue

70 toward scientific discovery (Shen et al., 2018). The main objectives of this study were: (i) to develop a modelling approach able to integrate hillslopes erosion processes into karstic transfer, and (ii) to evaluate the impact of different land use scenarios on SD variability at a WTP. This study proposed an original approach in order to predict the variability of the SD at a WTP in the Radicatel catchment (Normandy, France). We ~~took advantages of using~~ an existing expert-based GIS model (WaterSed), developed and successfully applied on the studied area, to simulate the impact of land use management on erosion and runoff.

75 The main idea was to predict, and extract SD entering connected sinkholes on the studied catchment and take the opportunity to use it as inputs for a data-driven model (i.e. DNN). Then, the coupled modelling approach was applied to multiple ~~designed storm~~ ~~project~~ (DSP) under different scenarios in order to predict SD variability at the WTP.

2 Study Site

2.1 Radicatel Water Treatment Plant

80 The study site is in the Pays de Caux (Normandy, France) on the right bank of the Seine river about 30 km from the Seine estuary (Fig. 1a). The climate is temperate with an average temperature of 11 °C. Annual precipitation ranges between 600 and 1100 mm with a rainy season occurring between October and May. The karst is typical of the geological setting of the lower Seine Valley. The karstic chalk plateaus of the North-Eastern side of the Normandy region are part of the western edge of the Paris Basin. The geology consists of Cenomanian to Campanian chalk overlaid by thick surficial formations. The major

85 formation is composed of clay-with-flints which results from the weathering of the chalk (Laignel, 2003), loess, and tertiary sands (Lautridou, 1985). The thickness of the formation overlying the chalk ranges from 5 to 10 m. Ground water infiltrates from the uplands of the chalk aquifer to the valleys via rapid transfer through a highly developed karstic network, and via slower drainage through the thick surficial formations. The catchment of Radicatel covers 106 km² and the WTP is located at the interface of the Seine alluvium and the karstic chalk (Fig. 1b.) Water is pumped through four different springs and seven

90 pumping well near the WTP (Chédeville, 2015). According to the information system for groundwater management in Seine-Normandy (http://sigessn.brgm.fr/), hydrogeological investigations reported seven sinkholes positively connected to the springs. The WTP of Radicatel is exploited by the Le Havre-Seine Métropole (LHSM) to supply Le Havre inhabitants.
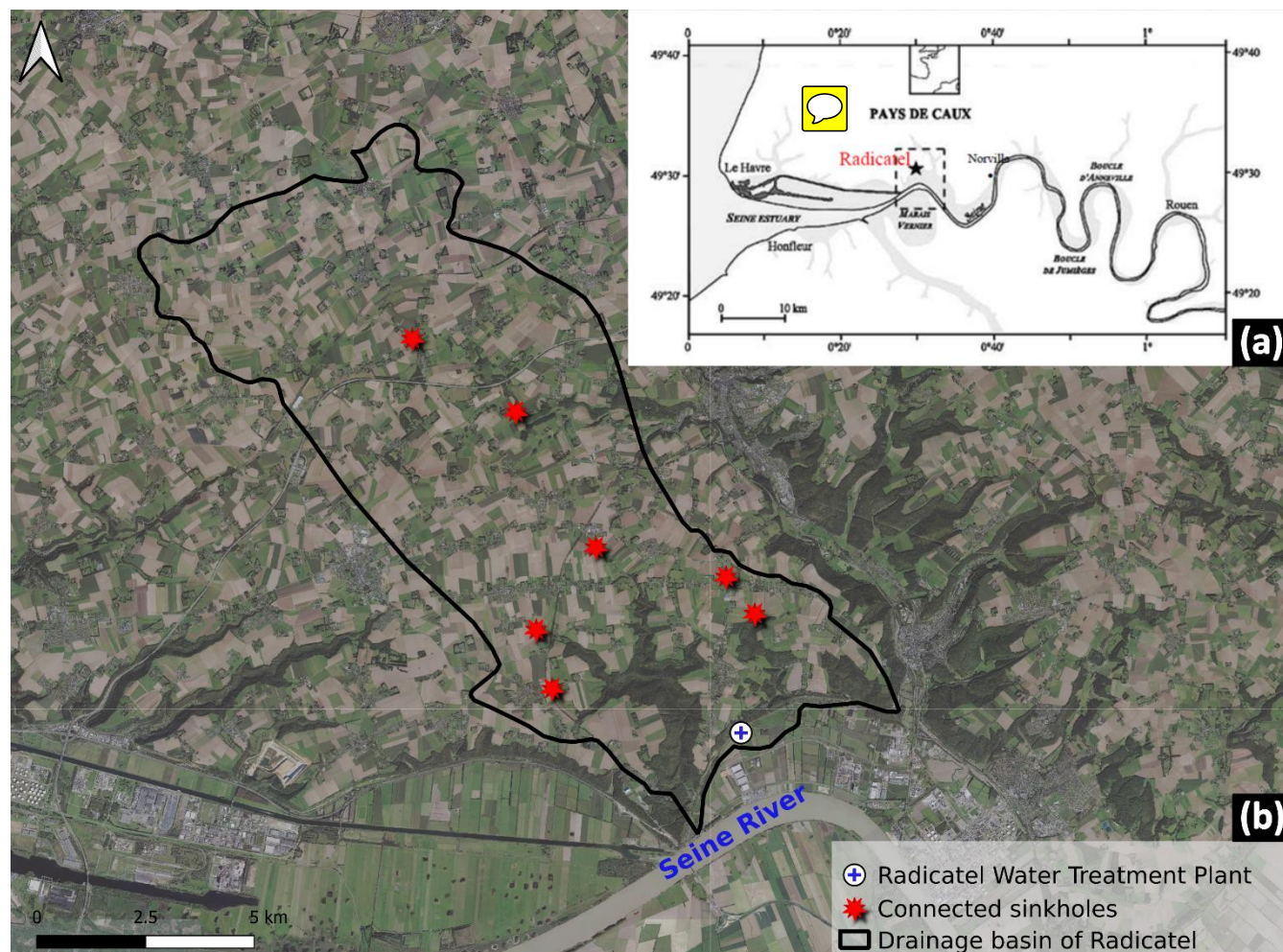
Figure 1: (a) Location of the study site in the lower Seine Valley (Normandy, France) on the right bank of the Seine River (Hanin, 2011), and (b) Location of the water treatment plant of Radicatel and the seven connected sinkholes. Background map was retrieved from the BD Ortho© – IGN.

2.2 Hydro-climatic data

At the Radicatel WTP, the mean pumping flow rate is estimated to 19733 m^3 d^{-1}, and the volume of water pumped in 2018 is approximately 7.2 million m^3. Turbidity (NTU) is measured with a nephelometer at the face of the pumping station and recorded since 1987 (Fig. 2). Maximal turbidity value is recorded every day ($\Delta t = 1$ d) and LHSM provided access to the entire turbidity time series (1987-2017). Incomplete periods or hydrologic years with missing data were discarded. Twenty-two hydrologic years with a complete time-series of turbidity were kept for the rest of the study. Cumulative daily rainfall (mm) from 1987 to 2017 were extracted from SAFRAN database with a spatial resolution of 8 km over the water catchment basin of Radicatel (Vidal et al., 2010).
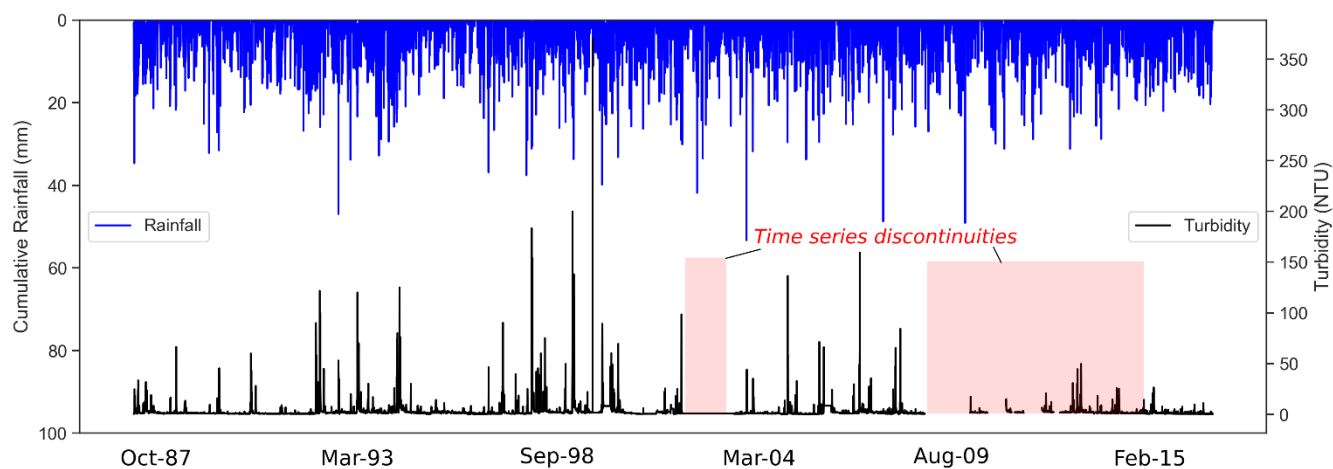
105

Figure 2: Cumulative daily rainfall (mm) extracted from SAFRAN database over the Radicatel water catchment basin and maximum daily turbidity (NTU) observed at the water treatment plant from 1987 to 2017.

3 Methodology

The proposed coupled modelling for the simulation of SD at WTP incorporates five different components that can be used
110   separately or as part of an integrated modelling framework. These components are described in detail in the following sections.

3.1 Data handling

Appropriate data handling can help address various concerns in DNN modelling, such as their ability of generalization beyond
~~their~~ training limits (Kourgialas et al., 2015). Moreover, coupling GIS and DNN modelling can require important
computational effort; therefore, the input data must be carefully selected. In this study, turbidity data distribution was explored
115   using scatter plot (Fig. A1). The input turbidity data was chosen so that it includes the best dispersion of values (0-370 NTU)
and a strong recurrence of extreme turbidity values (> 150 NTU). ==Thus, two significant hydrologic years (H12-H13; from
10/1/1998 to 9/30/2000) were selected, accounting for 731 daily events.== Thus, these two hydrologic years were selected as the
reference period for the calibration and training of the model. SD (kg d^{-1}) was assessed considering turbidity time series, mean
pumping flow rate at the Radicatel WTP and a mean sediment concentration resulting from field investigations (~1 mg L^{-1};
120   Hanin, 2011). In accordance with previous studies by Masséi et al. (2006) and Hanin (2011) in karstic environment in
Normandy, a lag of 1 day was applied to the SD time series to properly match the rainfall input. Erosion and runoff were
calculated with WaterSed model for 269 events to reduce computational efforts, considering that erosion and runoff occurs
only for significant rainfall events (P > 2.5 mm; threshold below which no effective rainfall is generated; and runoff and
sediment discharge entering connected sinkholes was set to 0).

3.2 Erosion and runoff modelling

The WaterSed model uses a raster-based distributed approach to model the spatial distribution of runoff and soil erosion within a catchment for a given rainfall event. The WaterSed model is an upgrade of the STREAM model (Souchère et al., 1998; Cerdan et al., 2001) simulating hydrological processes by conceptualizing each raster grid cell as a reservoir whose properties are calculated at the event-scale and by routing both water and sediment according the surface flow network. The WaterSed model requires six datasets to compute runoff and erosion for any location in the catchment:

- Digital Elevation Model (DEM) to extract slope and the runoff flow network,

- Stream network (to burn the stream network into DEM) and river width,

- Land cover and soil texture map to associate each land cover in the catchment with the appropriate soil surface characteristics,

- Decision tables, adapted for the local conditions, to associate each soil surface characteristic observed in the land cover or field with a steady-state infiltration rate, a Manning's roughness coefficient, a single potential sediment concentration and a soil erodibility value, and

- Rainfall events including total precipitation, antecedent moisture (48h) and effective rainfall duration.

The DEM (5m, BD Alti®) depressions were filled according the algorithm developed by Wang and Liu (2006). The stream network location and width were provided by the BD TOPO®. A land cover map was developed for 2016 by combining two national databases: the French Land Parcel Identification System (RPG) and the Soil Observatory of Upper Normandy (OSCOM). A soil texture map with three classes: clay, silt, and sand were derived from the Regional Soil Referential (RRP) with a precision of 1:250000. The parametrization consists of a characterization of the main parameters influencing runoff and infiltration in the studied context: soil surface crusting, surface roughness and crop cover. These soil surface characteristics were defined for each month and for each crop class according to the cropping calendar developed by Evrard et al. (2010) and Delmas et al. (2012). Steady-state infiltration and potential sediment concentration were assigned to each soil surface characteristics according to Cerdan et al. (2001) and Cerdan et al. (2002b). The WaterSed model requires Manning's roughness coefficient in order to compute flow velocity. Based on soil surface characteristics, Manning's values were derived from surface roughness (Morgan, 2013) and the percentage of crop cover (Gilley et al., 1991). Last, soil surface characteristics were also used to define the soil erodibility factor, varying in the [0-1] interval, by adapting table developed by Souchère et al. (2003a). Calibration parameters were extracted from a previous study (Landemaine, 2016; Landemaine et al., 2020b) conducted in the Austreberthe catchment, located 30 km east of the Radicatel catchment.

3.3 DNN Configuration

In this study, a multi-layer feed forward network (DNN) was built under Python version 3.6 using the high-level API Keras
155 (Chollet, 2015) and Tensorflow (Abadi et al., 2016) as a background engine. We used the rainfall time series (i.e. daily
cumulative rainfall (P); and 48h-antecedent rainfall (P_{48})) retrieved from SAFRAN database, and WaterSed modelling outputs
(runoff (R_{WS}) and sediment discharge (SD_{WS})) at connected sinkholes as input data for the DNN model. SD time series at the
Radicatel WTP was selected as output considering the two significant hydrologic years (H_{12}-H_{13}). Data (time series length n =
731) were split as a training set (70 %; n = 511) and a test set (30 %; n = 220). The training set was also split into training and
160 validation set to fine-tune the hyperparameters (70-30 %; n = 358-153). The optimum structure and configuration of the
network was found by a classical trial and error procedure (training-evaluation process through optimization of errors; Ortiz-
Rodriguez et al., 2013). When performing the DNN training, the number of iterations epoch was set to 15, and the batch size
to 1. Stochastic gradient descent (batch size = 1) was used to calculate error and update the model for each example in the
training dataset. The number of hidden layers and neurons depends on the characteristics of the input data, and there is no
165 specific rule for selecting these parameters (Le et al., 2019). The final structure of the DNN was composed of one input/output
layer and three hidden layers. We set 41 neurons in the hidden layers as follow: 30-10-1. Before training, input variables were
rescaled between 0 and 1 using normalization and re-transformed for the predictions using the normalization parameters. We
used the rectified linear (ReLU) as activation function for the first two nodes and linear activation function was set in the last
hidden layer. Mean square error (MSE) was chosen as loss function and the Adaptive moment estimation (Adam) was adopted
170 as the model optimization algorithm.

3.4 Performance evaluation

The choice of the training/test set remains arbitrary and may need to be evaluated to compute a robust estimate of model error.
With time series data, care must be taken when splitting the data in order to prevent data leakage. To address this issue, we
adapted a month-backward chaining nested cross-validation procedure, which provides an almost unbiased estimate of the true
175 error (Varma and Simon, 2006). The procedure contains an inner loop for parameter tuning, and an outer loop for error
estimation (see Fig. B1). The parameters that minimize error are chosen on the inner loop and we add an outer loop, which
splits the data into multiple training/test sets. Then, the error is averaged on each split to evaluate the overall performance of
the model. The performance of the model was evaluated through a range of statistical error measures including the coefficient
of determination (R^2), the Nash-Sutcliffe Efficiency (NSE), and the root mean square error (RMSE). The coefficient of
180 determination (R^2) ranges from 0 to 1 and describes the amount of observed variance explained by the model. A value of 1
suggests that the model can explain all the observed variance, whereas a value of 0 implies no correlation.

$$R^2 = \frac{(\sum_{i=1}^{n}(y_i - \bar{y})(y_i' - \bar{y}'))^2}{\sum_{i=1}^{n}(y_i - \bar{y})^2 \sum_{i=1}^{n}(y_i' - \bar{y}')^2} ,$$

(1)

Where y_i is the observed variable at time i, y_i' is the predicted variable at time i, $\bar{y}$ and $\bar{y}'$ the mean values of observed and predicted variable at time i, and n the number of observations.

185   The root mean square error (RMSE) corresponds to the standard deviation of the residuals (prediction errors). The residuals are a measure of the distance from the data points of the regression line. It evaluates how the predictions match to the observations, and values may range from no fit ($+\infty$) to perfect fit (0) based on the relative change of the data.

$$RMSE = \sqrt{\frac{\sum_{i=1}^{n}(y_i - y_i')^2}{n}}, \tag{2}$$

The Nash-Sutcliffe Efficiency (Nash and Sutcliffe, 1970), indicates the model's ability to predict variables different from the
190   mean, and gives the proportion of the initial variance accounted by the model. NSE values vary between $-\infty$ (poor model) and 1, indicating a perfect fit between observed and predicted values.

$$NSE = 1 - \frac{\sum_{i=1}^{n}(y_i - y_i')^2}{\sum_{i=1}^{n}(y_i - \bar{y})^2}, \tag{3}$$

3.5 Designed storm projects and land use scenarios

Five designed storm projects were constructed for the modelling approach based on expert knowledge and depth-duration-
195   frequency curves of the French Meteorological Survey (Météo-France) available from 1996-2006 on the studied area (Table 1). We considered winter events for low return period rainfall (0.5 and 2 year return period). In the studied region, low daily cumulative rainfall can lead to severe erosion by water runoff, due to saturated soils induced by heavy cumulated rainfall on the antecedent days (Le Bissonnais et al., 2002; Evrard et al., 2010). For higher return period (i.e. 10, 50, and 100 year return period) we considered spring events that are characterized by stronger rainfall intensities and can be particularly damaging in
200   this region (Evrard et al., 2007).

Table 1: Designed storm projects defined for the Radicatel catchment and considered for the simulations.

Return period (year)	Daily cumulative rainfall (mm)	6-min maximum intensity (mm h^{-1})	48h-antecedent rainfall (mm)	Season
0.5	19	25	45	Winter
2	31.4	25	45	Winter
10	51.9	45	0	Spring
50	74.7	45	0	Spring
100	87	45	0	Spring

Three land use change scenarios by 2050 were investigated and compared to a baseline land use scenario (2018). The scenarios were incorporated in the model in order to predict SD variability at the WTP and evaluate their impacts. All scenarios are
205   described below:

- Baseline scenario (S_base): This scenario served as a reference and was built considering ~~last~~ available land use data on the catchment (see section 3.3). Existing erosion control measures by 2018 were considered and extracted from regional database (BD CASTOR; http://bdcastor.fr/). The database contained 45 dams/retention ponds, 16 ponds, 1 fascine, and 4 hedges for the actual land use scenario on the Radicatel catchment, which have been included in the WaterSed model.

- Ploughing up of grassland (S_grass): For the 1970-2010 period in the studied region, we observed an average conversion rate of grasslands up to 1.8 % yr^{-1}. Extrapolation by 2050 lead to the conversion of 33% of actual existing grasslands. Grasslands were ploughed up based on a slope criterion, prioritizing those with ~~slight~~ slope, therefore mainly located on the plateau upstream of the catchment.

- Eco-engineering (S_engi): based on expert knowledge, 181 fascines and 13.1 ha of grass strips were implemented in addition to existing erosion control measures to mitigate runoff/erosion on the catchment and reduce rapid transfer via the connected sinkholes. Grass strips were deployed on the flow paths ~~nearby~~ the sinkholes. Fascines were deployed throughout the catchment, also on flow paths and along plot boundaries. The localization was optimized according to the baseline scenario simulations.

- Best farming practices (S_farm): This scenario promotes the adoption of farming practices improving infiltration on the catchment (increasing crop cover or delaying the formation of the slaking crust). 50 % of plots were randomly selected ~~and we applied a~~ 15 % increase in infiltration capacity, respecting the actual proportions of winter and spring crops on the catchment. The applied value was set based on the study of Maetens et al. (2012), who synthetized the reduction in erosion and runoff following different agricultural practices across Europe. According to their results, ~~the~~ 15 % increase in infiltration capacity ~~is~~ a ~~low case~~ assumption easily achieved through simplified cultural techniques (e.g. minimum tillage, no till, direct seeding, crop cover, etc.).

4 Results

4.1 Modelling the inputs

In order to fed the DNN, erosion and runoff were simulated with the WaterSed model for 269 rainfall events over the entire Radicatel catchment. We used the WaterSed parametrization that was carried out on the adjacent catchment (La Lézarde; Landemaine et al., 2020a) and that already proved to be valid on the same area of the Pays de Caux (Landemaine, 2016; Landemaine et al., 2020b) and Belgium (Baartman et al., 2020). For each event, WaterSed outputs (i.e. runoff (R_{WS}; m^3) and sediment discharge (SD_{WS}; kg d^{-1}) values) were extracted and summed over all positively connected sinkholes. Figure 3 shows that from October 1998 to September 2000, rainfall events led to a significant cumulative runoff and sediment discharge to the sinkholes (R_{WS} = 213225 m^3; SD_{WS} = 262806 kg). Most of the events occurred in spring (SD_{WS_spr} = 131672 kg; R_{WS_spr} = 94732 m^3) and winter (SD_{WS_win} = 88413 kg; R_{WS_win} = 62590 m^3). Sediment discharge and runoff occurred on the catchment

for only 126 events over the 269 simulated. 61 % of the SD_{WS} (i.e. 162168 kg) and 52 % of the R_{WS} (i.e. 110877 m^3) were transported during seven major events (i.e. 0.95 % of the time). Over the 126 events, the maximum R_{WS} and SD_{WS} reached 38471 m^3 and 38380 kg (μSD_{WS} = 2102 kg; μR_{WS} = 1705 m^3; σSD_{WS} = 5826 kg; σR_{WS} = 4437 m^3).
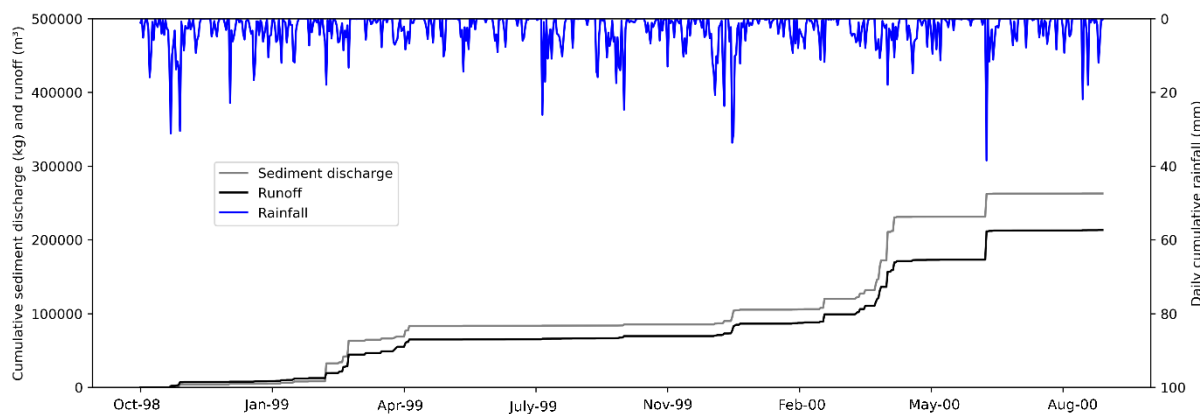
240

Figure 3: Cumulative sediment discharge (kg) and runoff (m^3) predicted by the WaterSed model, extracted and summed over all positively connected sinkholes from October 1998 to September 2000.

4.2 DNN: Calibration and Generalization

We used the runoff and sediment discharge predicted by the WaterSed model for the two selected hydrologic years. Predicted values of runoff and sediment discharge were extracted over the connected sinkholes and summed to be used as inputs for the DNN. The rainfall time series (P, P_{48}) available on the catchment were also considered as inputs. Turbidity time series recorded at the WTP was transformed into sediment discharge knowing the mean pumping flow rate at the Radicatel WTP, and considering a mean sediment concentration of 1 mg L^{-1} from field investigations made by Hanin (2011). Thus, sediment discharge at the WTP was considered as output of the DNN. The DNN was trained from October 1998 to February 2000 (*n* = 511 daily events). The remaining period from March 2000 to September 2000 was used as the test set (*n* = 220 daily events). Modelling results (Fig. 4) suggested a good agreement between observed and predicted SD at the WTP over the test set, with a NSE criterion reaching 0.82 and a RMSE around 383 kg. The temporal variability was also well reproduced. The results over the training set were slightly less efficient and reached a NSE of 0.6 and a RMSE of 420 kg. Overall results were above the classical threshold values for satisfactory model, defined between 0.5 < NSE < 0.65 in hydrological studies (Moriasi et al., 2007; Ritter et al., 2013). Over the investigated period, the cumulative SD observed at the WTP reached 158611 kg whereas the predicted cumulative SD reached 129253 kg (underestimation of 19 %). Comparing SD_{WS} and observed SD at the WTP attested a 60 % recovery rate from WaterSed outputs which was consistent with previous hydrogeological tracing results on connected sinkholes. Hanin (2011) suggested the existence of fast karstic connections between sinkholes and springs on Radicatel catchment, with a 62 % recovery rate. The recovery rate dropped to 50 % for the predicted SD. For the 126 events for which erosion and runoff occurred on the catchment, the cumulative amount for both observed and predicted SD was estimated to 88114 kg and 78870 kg respectively, suggesting that direct transfer accounts for 55-61 %. These results were

consistent with previous published results of Masséi et al. (2003) in same karstic environment (Norville catchment, Normandy, France), which evaluated the ~~part~~ of direct transfer ~~to~~ 73 % during erosive events.
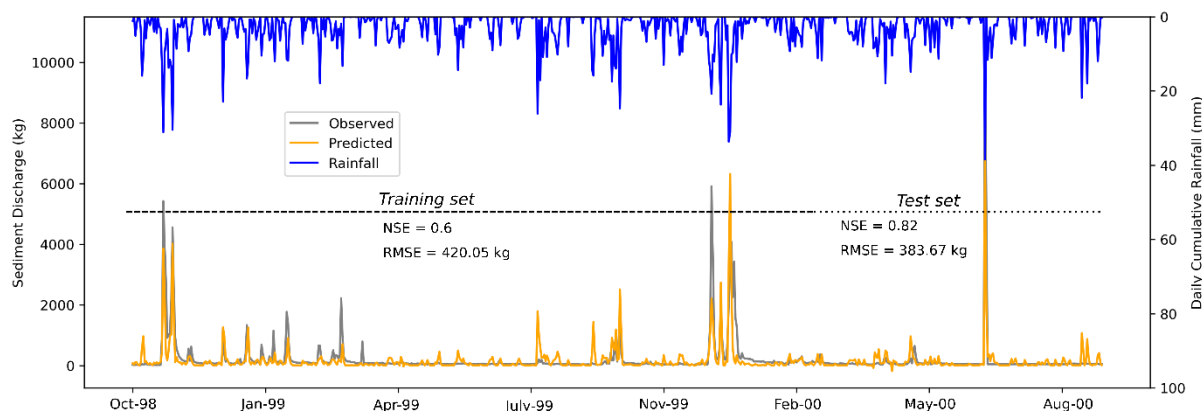
Figure 4: Observed and predicted sediment discharge (kg) at the water treatment plant using the DNN model.

The monthly-backward chaining nested cross-validation procedure made it possible to assess the generalization capacity of the DNN on a new data set. This procedure was repeated twelve times on all the data, while keeping at least one full hydrologic year as input for the modelling. The modelling results were less efficient than for the complete dataset but overall satisfactory (Fig. 5). The median NSE values for the training and the test sets was above ~~the lower limit of the threshold (Moriasi et al., 2007; Ritter et al., 2013)~~. The median RMSE values on the training and the test sets was in the same order of magnitude as for the complete dataset (300 – 500 kg). ~~Despite honorable performances, t~~he difficulties of the model to generalize suggested a classical problem in machine learning, the bias-variance dilemma (Geman et al., 1992). Ideally, the model should accurately reflect irregularities in the training data while generalizing to data testing, but it ~~is~~ not possible to ~~do~~ both at the same time. The higher NSE and lower RMSE values on training sets suggest a complex model with high variance and a reliable bias that represents the training data fairly well but present a learning risk on the test data. The model can thus represent part of the random noise of the learning dataset.
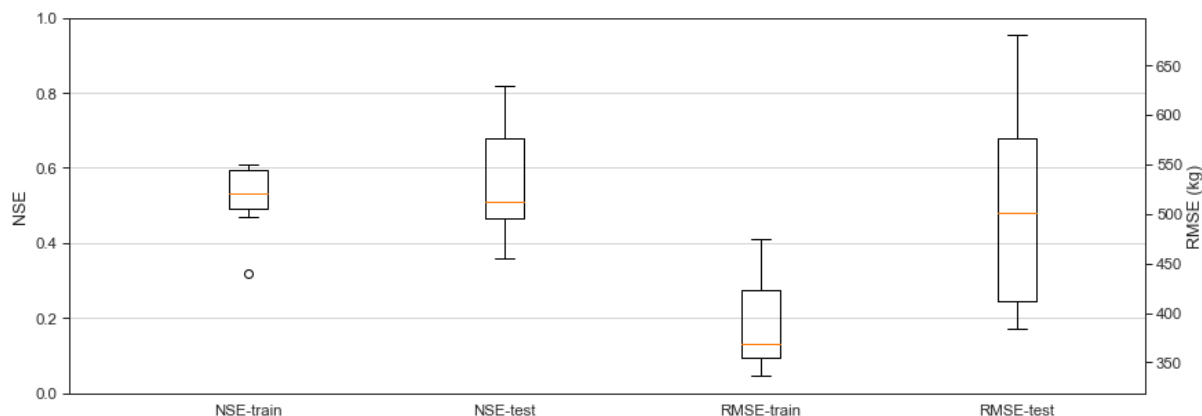
Figure 5: Boxplots of the performance metrics over the training and the test set using the month backward-chaining nested cross-validation.

4.3 Scenarios Predictions

Once the calibration was completed and the architecture of the DNN defined, we applied the model for all predefined scenarios. As a first step, and using the WaterSed model, we quantified SD_{WS} and R_{WS} at the connected sinkholes for the three additional scenarios and the five DSP, comparing them to the baseline scenarios (Fig. 6a-b). For the first scenario (S_grass), 33 % of grasslands were ploughed up, which led to an increase of the spatial extent of runoff generation on the catchment. SD_{S_grass} ranged from 8468 to 188264 kg for $P_{0.5}$ to P_{100}, which led to an average increase of 4.74 % compared to the results on the baseline scenario. The SD increase was maximal (+7.45 %) for the 10-years DSP. The increase in runoff was higher, with an average increase of 8.4 % on the five DSP, ranging from 2211 to 67097 m³. The second scenario (S_engi) considered the implementation of erosion control measures by 2050 (i.e. 181 fascines and 13.1 ha of grass strips), which led to a global decrease in sediment fluxes rates. Simulated SD_{S_engi} ranged from 1659 to 133458 kg to connected sinkholes, resulting in an average decrease of 44 %. This scenario was more effective on small return periods (i.e. 0.5 and 2-years), with a SD decrease between 79 and 55 %, respectively. Erosion control measures were less effective on the three other DSP, with a decrease ranging from 25 to 34 %. The effects on runoff was not significant, with an average decrease of 7 %. These results were not surprising considering that this management plan only included 13.1 ha of grass strips, and the main interest of the fascines lies in their ability to trap suspended sediments, especially the coarsest elements (AREAS, 2012). The last scenario (S_farm) considered the adoption of good farming practices (i.e. +15 % infiltration capacity) on 50 % of the plots. It can be observed that this scenario significantly reduced sediment production on the hillslopes (Fig. 7a-b). The simulated SD_{S_farm} ranged from 741 to 134001 kg for an average decrease of 49 % compared to the baseline scenario results. The simulated values on water runoff ranged from 720 to 47442 m³. This scenario was more effective in reducing SD and runoff, in average, than the eco-engineering scenario. The SD decrease induced by good farming practices ranged from 25 to 90 % at the connected sinkholes.
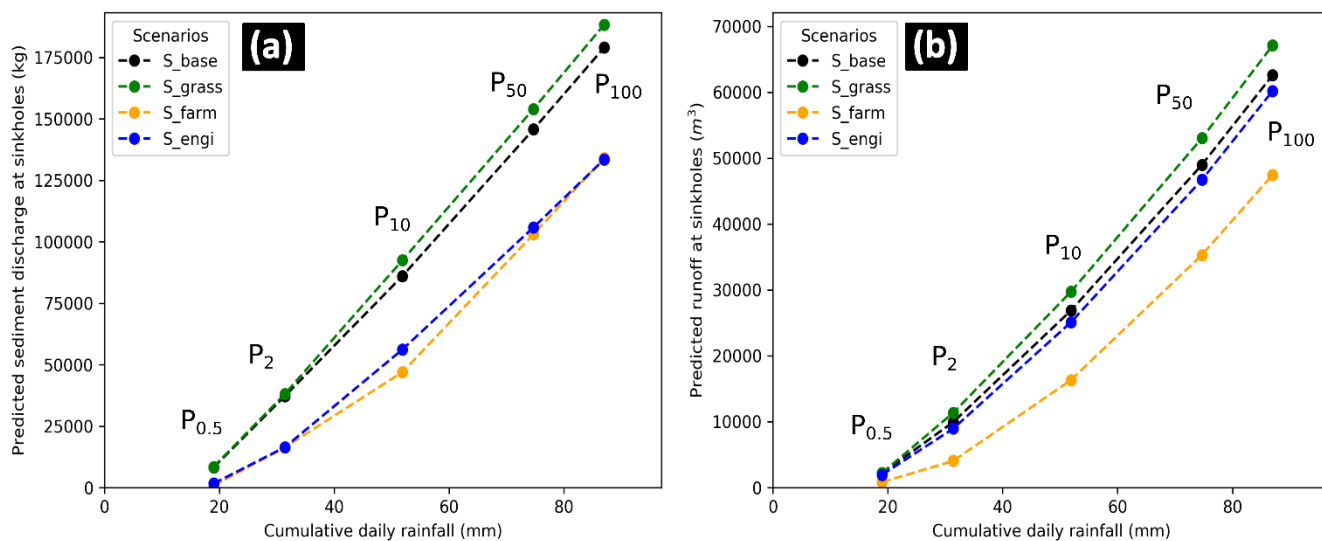
300

Figure 6: WaterSed modelling results according to the five designed storm project for the four scenarios: (a) Predicted sediment discharge (kg) and (b) runoff (m³) extracted and summed at the connected sinkholes on the Radicatel catchment. (S_base = baseline scenario in 2018; S_grass = 33 % of grasslands ploughed up; S_farm = +15 % infiltration capacity on 50 % of the plots; S_engi = implementation of 181 fascines and 13.1 ha of grass strips).
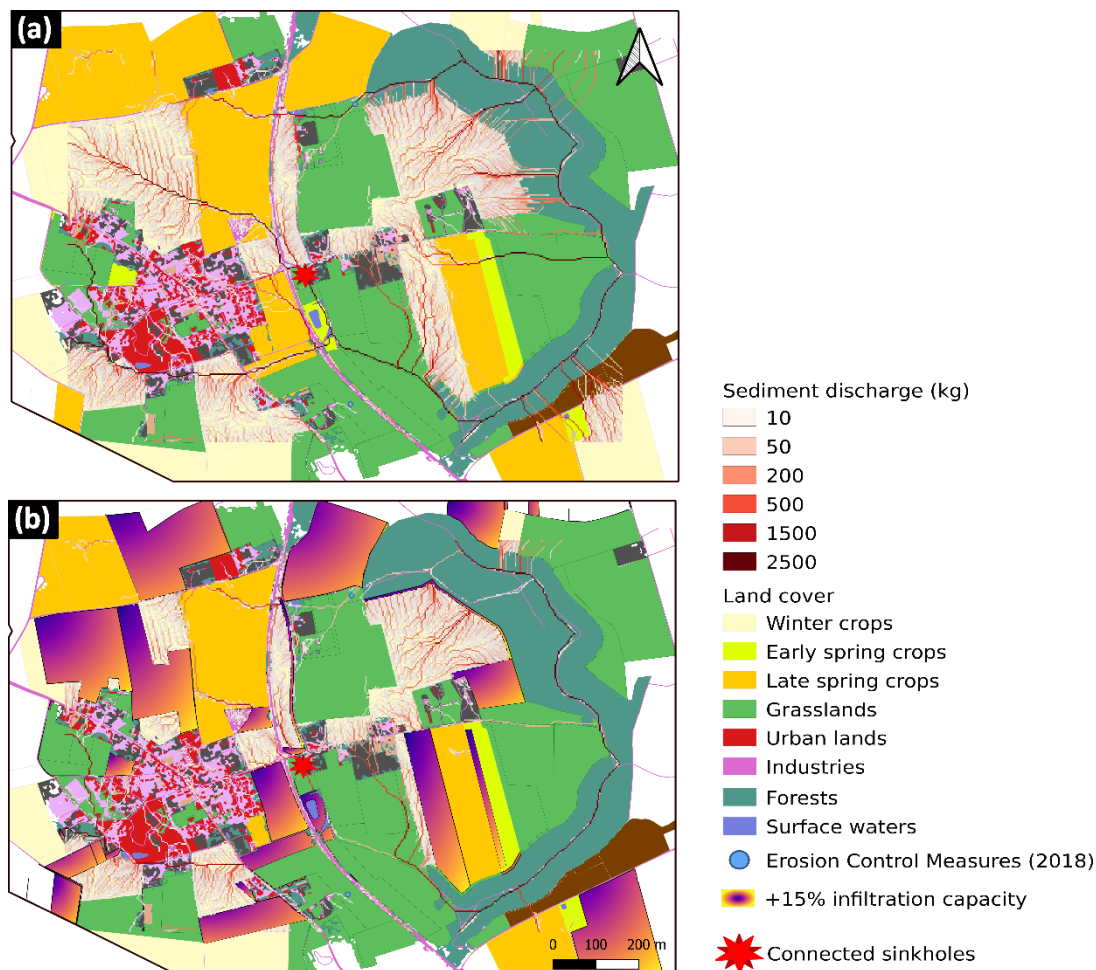
Figure 7: Mapping of flow path and sediment discharge for (a) the baseline scenario, and (b) the scenario including an increase of 15% of the infiltration capacity on selected plots, for the 100-year return period designed storm project on the Radicatel catchment.

DSP characteristics and predicted SD/runoff by the WaterSed model at connected sinkholes, and for all scenarios, were injected as inputs in the DNN model. On the baseline scenario, predicted SD at the WTP ranged from 576 to 12200 kg (see section 4.2), and the Fig. 8 shows the global trends of the scenarios modelling results. For the S_grass scenario, predicted SD at the WTP were slightly higher than the baseline scenario, reaching 12894 kg for the 100-years DSP. This scenario resulted in an average increase of 4.5 % for the SD at the WTP. The SD increase was less significant on small return periods (+0.42-3.29 %) than longer return periods (+5.68-6.82 %). On the third scenario (S_engi), the modelling results suggested a significant SD decrease at the WTP. The predicted SD ranged from 515 to 9810 kg that led to an average decrease of 25.4 %. The SD reduction was particularly effective on the 2-years DSP reaching a decrease of 44.7 %. The smallest SD reduction was observed for the 0.5 years DSP (10 %) and ranged from 19 to 30 % on longer return periods. These results were consistent with those found by Fournier et al. (2008), who showed by a parametric interpolation model that erosion control measures at connected sinkholes on the Caumont aquifer led to a 36 % decrease of the turbidity in the Varras WTP (Normandy, France). The last scenario

(S_farm) was the more efficient with a predicted SD ranging from 223 to 9165 kg and a high average decrease of 43 %. The

320   SD reduction ranged from 28.9 to 61.3 % and was the more efficient for the 0.5 and 2-years return period (55.6-61.3 %).
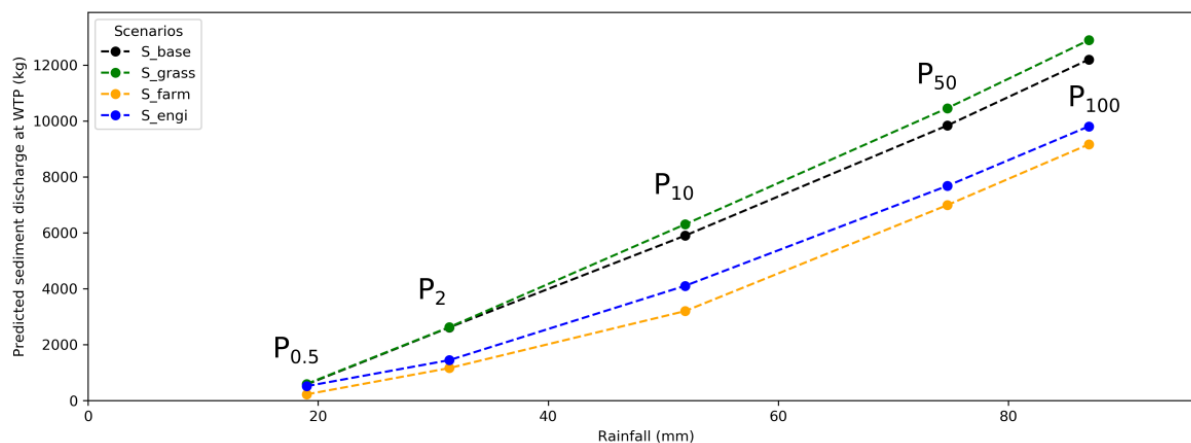
Figure 8: Predicted sediment discharge (kg) for designed storm project and all scenarios at the Radicatel water treatment plant (WTP) using DNN model (S_base = baseline scenario in 2018; S_grass = 33 % of grasslands ploughed up; S_farm = +15 % infiltration capacity on 50 % of the plots; S_engi = implementation of 181 fascines and 13.1 ha of grass strips).

325   ## 5 Discussion

5.1 Coupled modelling approach: strength and uncertainties

The original modelling approach developed in this study allowed the coupling of surface and subsurface sediment transfer processes. As karstic processes are complex and difficult to model due to the lack of knowledge of their geometry, the coupling of a process-based GIS model and a data-driven model (i.e. DNN) proved to be a powerful tool. This approach makes it easy

330   to assess the impact of different land-use scenarios on drinking water quality at drinking water treatment plants. Despite very encouraging results, one may noticed that the coupled model was trained on only two years of complete selected measurements, and therefore may not have captured the full distribution of possible cumulative daily rainfall on the catchment and/or turbidity values at the drinking water treatment plant. To ensure that the model may not have a weakness on the representativeness of extremes events, we performed an additional evaluation using the Generalized Extreme Value Distribution (GEV) that was

335   largely applied to extreme events such as rainfall or river discharges (Carreau et al., 2013; De Michele and Avanzi, 2018). We applied the GEV distribution to SD time series at the WTP of Radicatel. The maximum annual SD observed at the WTP was extracted for all complete hydrologic years (i.e. annual maximal blocks; $n = 22$) and the frequency distribution was assessed using the package 'extRemes' under R software (R Development Core Team, 2008; Gilleland and Katz, 2016; see Fig. C1). We compared the SD simulated at the WTP by the DNN to the distribution values predicted by the GEV. Firstly, we simulated

340   overall SD for the baseline scenario at the connected sinkholes and for the five DSP, using the WaterSed model. Then, we used these modelling results as inputs for the DNN model and applied it to the five DSP. Secondly, we compared the results with the calculated GEV distribution (Fig. 9). The SD predicted at the WTP by the DNN model was in good agreement with

the ~~distribution calculated~~ by GEV even ~~with~~ a high dispersion for highest return period. ~~Even if it is~~ well known that deep

learning-based methods may result~~s~~ in weak performance for extreme events (Zhang et al., 2019), the results obtained here

345 give confidence in the model's ability to simulate ~~extreme events thanks to a careful selection of input data~~. The degree of

confidence in the model's output could be improved with longer time series. One limitation of the presented coupled approach

is the data availability and its ability to be validated at other study sites, as the turbidity data backup are not always properly

done in all WTP. ==From now on, the drinking water supplier should keep turbidity records to allow the application of these==

==data-driven models, with the guarantee of a quality control to avoid interruptions in the time series.==
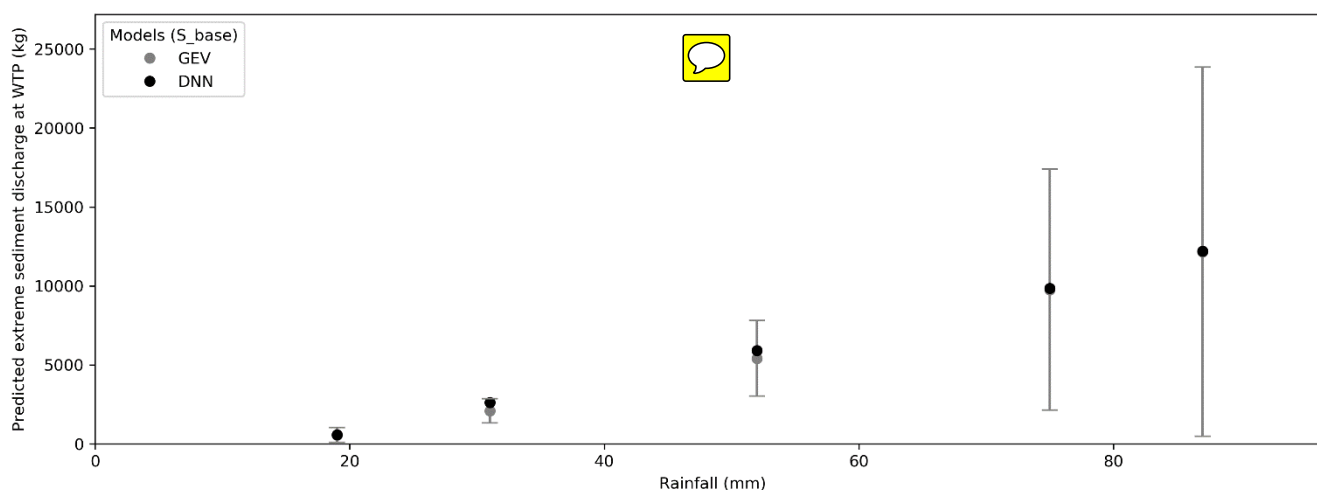
350

Figure 9: Predicted sediment discharge (kg) at the water treatment plant of Radicatel for the five designed storm project and the land use baseline scenario by (1) Generalized Extreme Values distribution, and (2) DNN modelling. The grey bars represent the 95% confidence intervals.

5.2 Implications for Future Land Use Strategies

355 The modelling results in this study suggest that two different land use strategies (i.e. increase of capacity infiltration and eco-engineering) can significantly reduce the SD incoming to connected sinkholes during extreme rainfall events (up to 90 %), and

therefore, decrease the SD at the WTP (from 10 to 61%). The first strategy leads to a decrease in sediment production through

simplified cultural techniques, while the second affects transfer processes. The adoption of better farming practices (e.g

increase of crop cover, no-tillage, reduced tillage) inducing an increase of 15 % of the capacity infiltration on 50 % of the

360 agricultural plots ~~on~~ the catchment, appears to be slightly more efficient than the implementation of eco-engineering

infrastructures (181 fascines + 13.1 ha of grass strips) for reducing SD at the WTP. These results thus show that it is more

interesting to adopt a land use strategy aimed at reducing hydro-sedimentary production directly on cultivated plots than

transfer processes on the catchment, but these strategies could be combined. Additional simulations integrating both effects of

best farming practices on cultivated plots and the implementation of eco-engineering infrastructures show a tenfold effect. As

365 illustrated in Fig. 10, the coupling of the two strategies makes it possible to reduce significantly the SD at the WTP. The

combined effect will not add up, but we can expect an improved decrease in sediment discharge at the WTP from 40 % to 80

%. Both land use strategies can also provide interesting effects on biodiversity and ecosystem services (Posthumus et al., 2015) and/or can improve soil resilience and promote sustainable agriculture (Lal, 2014). Public policies leading to the implementation of erosion control measures can be economically viable and efficient (Patault et al., 2020). Even if some
370 simplified cultural techniques may imply negative returns for farmers, they may be eligible for agri-environment payments (Posthumus et al., 2015). The implementation of these land use strategies may also require specific maintenance to keep their initial performance (Frankl et al., 2018) or specific training and machines for farmers.
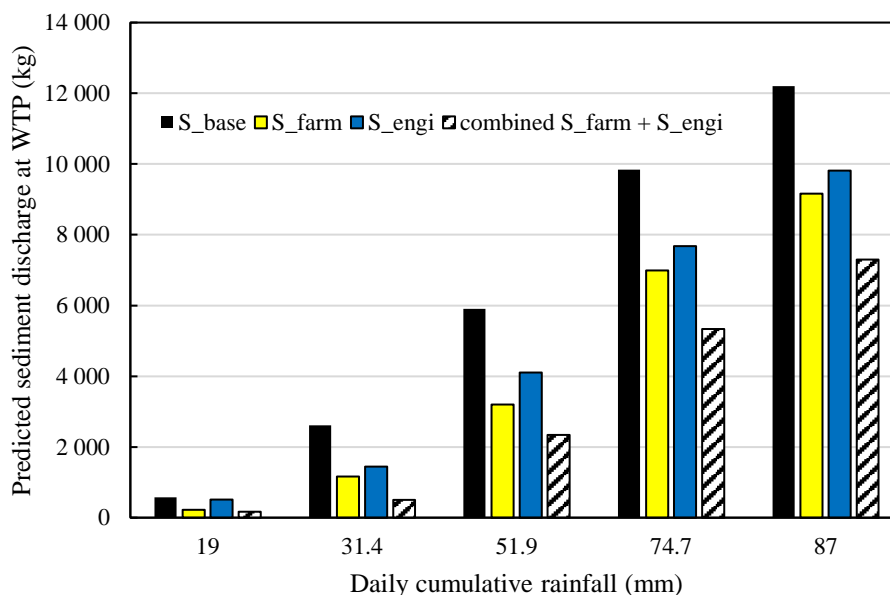
Figure 10: Comparison of predicted sediment discharge (kg) at the Radicatel water treatment plant by the DNN modelling for the
375 **baseline scenario, the two land use scenarios including best farming practices or the implementation of eco-engineering infrastructure, and the combination of both strategies.**

According to the simulations, the ploughing up of 33 % of grasslands for the benefit of agricultural plots on the catchment by 2050, will not increase significantly the SD at the WTP (less than 5 % in average). Our simulations just extended the current trend observed in the studied region. Despite all, some precautions must be taken regarding the results of this scenario which
380 could be higher or lower, depending on the localization of the ploughed-up plots. Same observations were made by Souchère et al. (2005) who suggested, according to their results, that the efficiency of all developments in reducing erosion and runoff is linked to their location within the catchment. Indeed, it is well known that hydrologic connectivity may lead to increments in runoff (Appels et al., 2011).

385

5 Conclusions

390 In this study, a new coupled modelling approach was developed in order to help decision-makers choosing an adapted erosion and runoff management strategy to reduce the impact of sediment discharge on drinking water supply. Expert-based GIS model (WaterSed) was used to simulate erosion and runoff at connected sinkholes on the Radicatel catchment (Normandy, France) and was coupled to a data-driven model (i.e. DNN) to simulate karstic transfer. This new approach can be easily implemented, does not require a knowledge of the geometry of the karstic system studied, and demonstrated the values of understanding

395 hillslopes erosion and runoff processes to model hydro-sedimentary in karstic systems. Our modelling results suggest that the coupled model performed well during the calibrating phase. The coupled model was able to generalize on unknown datasets through an adapted monthly backward chaining nested cross-validation procedure, but the results are just slightly over the threshold limit and suggest that more research should be done for the application on other catchments. The results also suggest that a land use change scenario considering the adoption of simplified cultural techniques can significantly reduce sediment

400 discharge at the water treatment plant (up to 61%). This scenario also performed the one who considered the implementation of eco-engineering control measures reducing erosion and runoff on the catchment (up to 45% at the water treatment plant). The coupling of the two cited land use strategies has proven to be the most effective since it operates both on the hydro-sedimentary production and transfer processes (decreasing SD at WTP from 40 to 80 %). Finally, ploughing up actual grasslands on the catchment will not increase significantly sediment discharge at the water treatment plant. In the framework

405 of this study, we can consider that the results might be different considering a different spatial organization of grasslands on the catchment and we suggest conducting a specific study on this hypothesis.

Appendix A: Scatter plot of turbidity time series
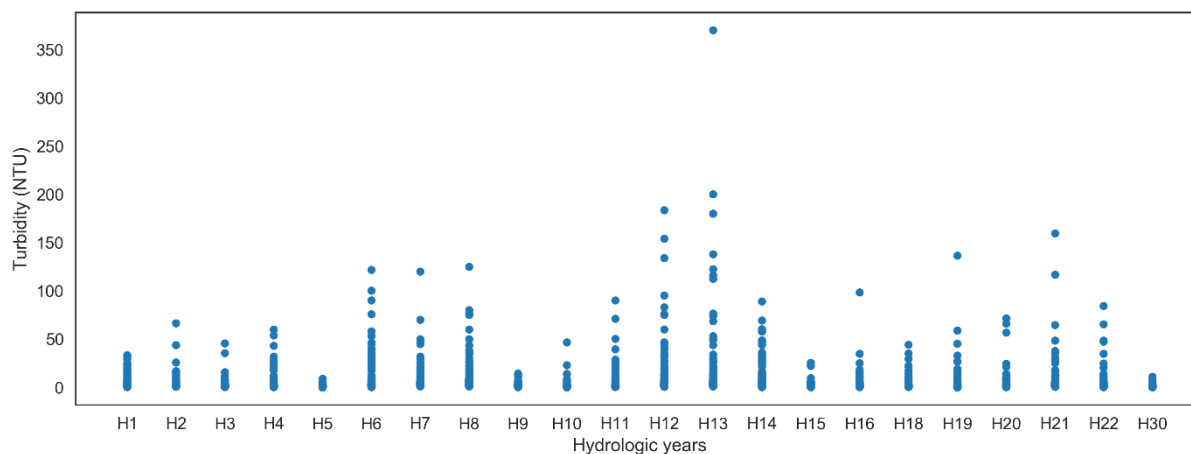
Figure A1: Scatter plot of turbidity time series recorded at the water treatment plant in the Radicatel catchment, Normandy, France.

Appendix B: Month-backward chaining nested cross-validation
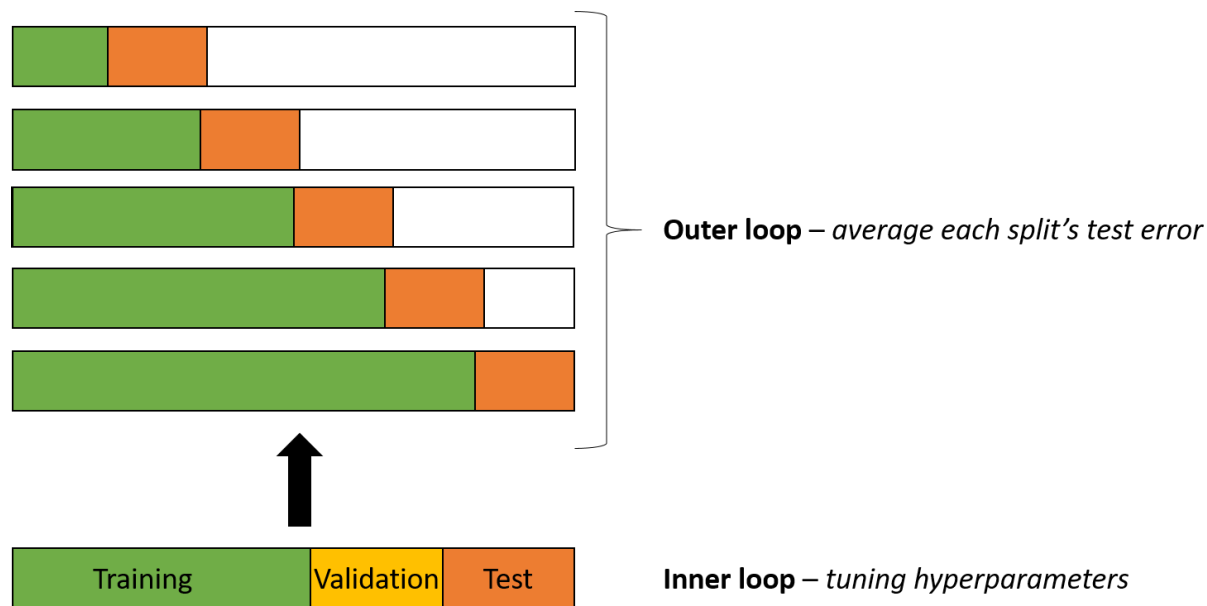
Figure B1: Month-backward chaining nested cross-validation procedure developed to test the generalization capacity of the model.

Appendix C: Generalized Extreme Values Distribution

415
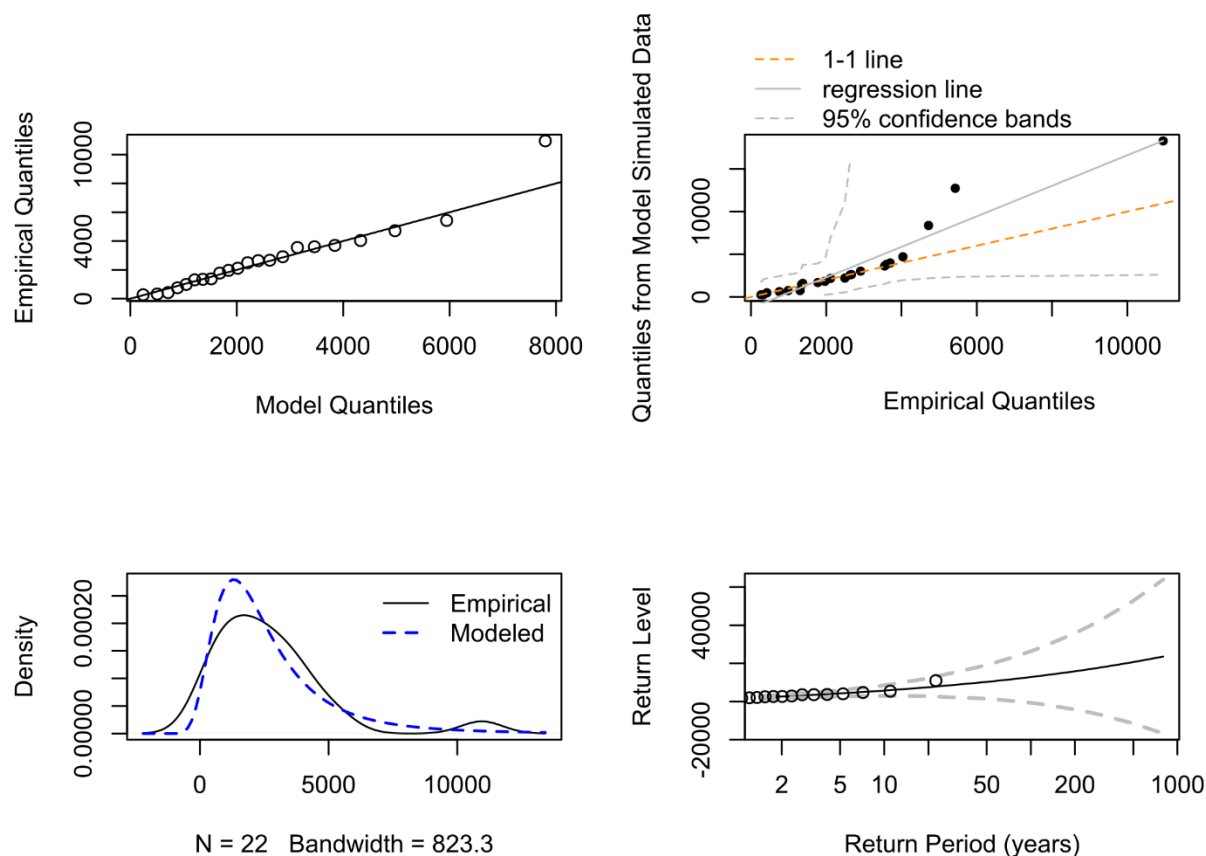
Figure C1: Generalized Extreme Values distribution modeled with the 'exTremes' R package on the sediment discharge time series (22 hydrologic years) at the water treatment plant in the Radicatel catchment.

Author contribution

Conceptualization EP, MF, BL, VL, OC, JFO, JL, AS; Formal analysis EP, VL; Funding acquisition BL, OC, JFO;

420   Investigation EP, VL, JL, AS; Methodology EP, MF, VL; Project administration MF, BL, OC, JFO; Software EP, VL; Supervision EP, VL; Validation EP, VL, MF, OC; Visualization EP; Writing – original draft EP, VL, MF, OC; Writing – review and editing

Competing interests

The authors declare that they have no conflict of interest.

Acknowledgments

This study is based on research undertaken as part of EVAPORE project "EVAluation de l'efficacité des POlitiques publiques pour les actions visant à REduire les impacts du ruissellement" to evaluate efficiency of public policy to reduce erosion and runoff impacts in Normandy, France. Authors are thankful to the University of Rouen, AREAS, BRGM, and Seine-Normandy Water Agency who co-founded this project. Authors are also thankful to the LHSM 'Le Havre Seine Métropole' who provided access to their data.

References

Abadi, M., Agarwal, A., Barham, P., Brevdo, E., Chen, Z., Citro,C., Corrado, G. S., Davis, A., Dean, J., Devin, M., Ghemawat, S., Goodfellow, I., Harp, A., Irving, G., Isard, M., Jia, Y., Jozefowicz, R., Kaiser, L., Kudlur, M., Levenberg, J., Mane, D., Monga, R., Moore, S., Murray, D., Olah, C., Schuster, M., Shlens, J., Steiner, B., Sutskever, I., Talwar, K., Tucker, P., Vanhoucke, V., Vasudevan, V., Viegas, F., Vinyals, O., Warden, P., Wattenberg, M., Wicke, M., Yu, Y., and Zheng, X. (2016). TensorFlow: Large-Scale Machine Learning on Heterogeneous Systems, available at: https://www.tensorflow.org/

Appels, W.M., bogaart, P.W., van der Zee, S.E.A.T.M. (2011). Influence of spatial variations of microtopography and infiltration on surface runoff and field scale hydrological connectivity. Advances in Water Resources, 34(2), 303-313 pp. https://doi.org/10.1016/j.advwatres.2010.12.003

AREAS (2012). Fascines & Haies pour réduire les effets du ruissellement érosif. Caractérisation de l'efficacité et conditions d'utilisation. 68p.

ARS (2013). Bilan 2013 de la qualité des eaux destinées à la consommation humaine et la protection des captages en Seine-Maritime. https://www.normandie.ars.sante.fr/sites/default/files/2017-03/bilan_76_qualite_eau_2013.pdf

Bai, Y., Chen, Z., Xie, J., Li, C. (2016). Daily reservoir inflow forecasting using multiscale deep feature learning with hybrid models. Journal of Hydrology, 532, 193-206 pp.

Baartman, J.E.M., Nunes, J.P., Masselink, R., Darboux, F., Bielders, C., Degre, A., Cantreul, V., Cerdan, O., Grangeon, T., Fiener, P., Wilken, F., Schindewolf, M., Wainwright, J. (2020). What do models tell us about water and sediment connectivity?, Geomorphology. https://doi.org/10.1016/j.geomorph.2020.107300

BRGM (2017). Analyse de l'érosion des sols sur le vignoble champenois de la Marne. BRGM/RP-66688-FR. Février 2017.

Carreau, J., Neppel, L., Arnaud, P., Cantet, P. (2013). Extreme rainfall analysis at ungauged sites in the south of France: Comparison of three approaches. Journal de la Société Française de Statistique, 154(2), 119-138 pp.

Cerdan, O., Souchère, V., Lecomte, V., Couturier, A., Le Bissonnais, Y. (2001). Incorporating soil surface crusting processes in an expert-based runoff model: Sealing and transfer by runoff and erosion related to agricultural management. Catena, 46, 189-205 pp. https://doi.org/10.1016/S0341-8162(01)00166-7

Cerdan, O., Le Bissonnais, Y., Couturier, A., Saby, N. (2002b). Modelling interrill erosion in small cultivated catchments. Hydrol. Process., 3226, 3215-3226 pp. https://doi.org/10.1002/hyp.1098

Chédeville, S. (2015). Etude de la variabilité du fonctionnement hydro-sédimentaire des karsts de l'Ouest du Bassin de Paris à partir de la comparaison des remplissages sédimentaires karstiques anciens, actuels et du signal turbide des eaux souterraines. Thèse de doctorat, Université de Rouen-Normandie, France, 458p.

Chollet, F. (2015). Keras, available at https://github.com/fchollet/keras

Delmas, M., Pak, L.T., Cerdan, O., Souchère, V., Le Bissonnais, Y., Couturier, A., Sorel, L. (2012). Erosion and sediment budget across scale : a case study in a catchment of the European loess belt. J. Hydrol. 420, 255-263 pp. https://doi.org/10.1016/j.jhydrol.2011.12.008

De Michele, C. & Avanzi, F. (2018). Superstatistical distribution of daily precipitation extremes: A worldwide assessment. Scientific Reports, 8:14204; doi: 10.1038/s41598018-31838-z

De Vente, J., Poesen, J., Verstraeten, G., Govers, G., Vanmaercke, M., Van Rompaey, A., Arabkhedri, M., Boix-Fayos, C. (2013). Predicting soil erosion and sediment yield at regional scales: Where do we stand ? Earth-Sciences reviews, 127, 16-29 pp. https://doi.org/10.1016/j.earscirev.2013.08.014

Evrard, O., Bielders, L.C., Vandaele, K., van Wesemael, B. (2007). Spatial and temporal variation of muddy floods in central Belgium, off-site impacts and potential control measures. Catena, 70(3), 443-454 pp. https://doi.org/10.1016/j.catena.2006.11.011

Evrard, O., Nord, G., Cerdan, O., Souchère, V., Le Bissonnais, Y., Bonté, P. (2010). Modelling the impact of land use change and rainfall seasonality on sediment export from an agricultural catchment of the northwestern European loess belt. Agriculture, Ecosystems and Environment, Elsevier Masson, 138(1-2), 83-94 pp. https://doi.org/10.1016/j.agee.2010.04.003

Fournier, M., Mouhri, A., Ratajczak, M., Rossi, A., Slimani, S., Mesquita, J. (2008). Fonctionnement hydrogéologique de l'aquifère de Caumont et incidence des aménagements de bassin versant sur la qualité des eaux du forage des Varras. https://www.unicaen.fr/m2c/IMG/pdf/rapportsersaep.pdf?262/447a7b605f6dbc8a8df025b439812a0bc73d39bf

Frankl A., Prêtre, V., Nyssen, J., Salvador, P-G. (2018). The success of recent land management efforts to reduce soil erosion in northern France. Geomorphology, 303, 84-93 pp. https://doi.org/10.1016/j.geomorph.2017.11.018

Geman, S., Bienenstock, E., Doursat, R. (1992). Neural networks and the bias/variance dilemma. Neural Computation, 4, 1-58 pp.

Gilley, J.E., Kottwitz, E.R., Wieman, G.A. (1991). Roughness coefficients for selected residue materials. J. Irrig. Drain. Eng. 117, 503-514 pp.

Gilleland, E. & Katz, R.W. (2016). extRemes 2.0: An extreme Value Analysis Package in R. Journal of Statistic Software, 72(8), 1-39 pp; doi:10.18637/jss.v072.i08

460

465

470

475

480

485

Hafeez, S., Sing Wong, M., Chak Ho, H., Nazeer, M., Nichol, J., Abbas, S., Tang, D., Ho Lee, K., Pun, L. (2019). Comparison of machine learning algorithms for retrieval of water quality indicators in case-II waters: a case study of Hong-Kong. Remote Sensing, 11, 617, https://doi.org/10.3390/rs11060617

Hanin, G. (2011). Contrôles structural et hydrogéologique sur la dynamique d'un champ captant en contexte crayeux karstique et sa sensibilité aux variations du signal climatique: Implications en matière de vulnérabilité de la ressource. PhD thesis, University of Rouen-Normandy, France, 320p.

Hartmann, A., Goldscheider, N., Wagener, T., Lange, J. and Weiler, M. (2014). Karst water resources in a changing world: Review of hydrological modeling approaches. Rev. Geophys., 52, 218-242, https://doi.org/10.1002/201RG000443

Hu, C., Wu, Q., Jian, S., Li, N., Lou, Z. (2018). Deep learning with a long short-term memory networks approach for rainfall-runoff simulation. Water, 10, 1543; doi:10.3390/w10111543

Jourde, H., Masséi, N., Mazzilli, N., Binet, S., Batiot-Guilhe, C., Labat, D., Steinmann, M., Bailly-Comte, V., Seidel, J-L., Arfib, B., Charlier, J-B., Guinot, V., Jardani, A., Fournier, M., Aliouache, M., Babic, M., Bertrand, C., Brunet, P., Boyer, J-F., Bricquet, J-P., Camboulive, T., Carrière, S-D., Celle-Jeanton, H., Chalikakis, K., Chen, N., Cholet, C., Clauzon, V., Dal Soglio, L., Danquigny, C., Défargue, C., Denimal, S., Emblanch, C., Hernandez, F., Gillon, M., Gutierrez, A., Hidalgo Sanchez, L., Hery, M., Houillon, N., Johannet, A., Jouves, J., Jozja, N., Ladouche, B., Leonardi, V., Lorette, G., Loup, C., Marchand, P., de Montety, V., Muller, R., Ollivier, C., Sivelle, V., Lastennet, R., Lecoq, N., Maréchal, J-C., Perotin, L., Perrin, J., Petre, M-A., Peyraube, N., Pistre, S., Plagnes, V., Probst, J-L., Simler, R., Stefani, V., Valdes-Lao, D., Viseur, S., Wang, X. (2018). SNO KARST: A French network of observatories for the multidisciplinary study of critical zone processes in karst watersheds and aquifers. Vadose Zone J. 17:180094. https://doi.org/10.2136/vzj2018.04.0094

Kourgialas, N.N., Dokou, Z., Karatzas, G.P. (2015). Statistical analysis and ANN modeling for predicting hydrological extremes under climate change scenarios: The example of a small Mediterranean agro-watershed. Journal of Environmental Management, 154, 86-101 pp.

Kratzert, F., Klotz, D., Brenner, C., Schulz, K., Herregger, M. (2018). Rainfall-runoff modelling using Long Short-Term Memory (LSTM) networks. Hydrol. Earth Syst. Sci., 22, 6005-6022 pp.

Laflen, J.M., Lane, L.J., Foster, G.R. (1991). WEPP: a new generation of erosion prediction technology. Journal of Soil and Water Conservation, 46, 34-38 pp.

Laignel, B. (2003). Caractérisation et dynamique érosive de systèmes géomorphologiques continentaux sur substrat crayeux. Exemple de l'Ouest du Bassin de Paris dans le contexte Nord-Ouest Européen, mémoire HDR, 138p.

Lal, R. (2014). Soil conservation and ecosystem services. International Soil and Water Conservation Research. 2(3), 36-47 pp. https://doi.org/10.1016/S2095-6339(15)30021-6

Landemaine, V. (2016). Erosion des sols et transferts sédimentaires sur les bassins versants de l'Ouest du bassin de Paris: analyse, quantification et modélisation à l'échelle pluriannuelle. PhD thesis. University of Rouen-Normandy, France, 236p.

Landemaine, V., Soulignac, A., Cerdan, O. (2020a). Analyse coût-bénéfice des actions de lutte contre le ruissellement et l'érosion des sols sur le bassin de la Lézarde. Rapport final. BRGM/RP-69650-FR, 142p.

Landemaine, V., Cerdan, O., Grangeon, T., Vandromme, R., Laignel, B., Evrard, O., Salvador-Blanes, S., Laceby, P. (2020b). Saturation-excess overland flow in the European loess belt: An underestimated process? In prep.

Lautridou, J-P. (1985). Le cycle périglaciaire pléistocène en Europe du Nord-Ouest et plus particulièrement en Normandie. PhD thesis, University of Caen, France, 908p.

Le, X-H., Ho, H.V., Lee, G. & Jung, S. (2019). Application of Long Short-Term Memory (LSTM) Neural Network for Flood Forecasting. Water, 11, 1387 ; https://doi.org/10.3390/w11071387

Le Bissonnais, Y., Thorette, J., Bardet, C., Daroussin, J. (2002). L'érosion hydrique des sols en France. Rapport INRA-IFEN, 106p. http://eduterre.ens-lyon.fr/thematiques/sol/degradation-du-sol/erosion-hydrique-2002-br.pdf

Maetens, W., Poesen, J., Vanmaercke, M. (2012). How effective are soil conservation techniques in reducing plot runoff and soil loss in Europe and the Mediterranean ? Earth-Science Rev. 115, 21-36 pp. https://doi.org/10.1016/j.earscirev.2012.08.003

Mangin, A. (1984). Pour une meilleure connaissance des systèmes hydrologiques à partir des analyses corrélatoire et spectrale. Journal of Hydrology, 67 (1-4), 25-43 pp.

Masséi, N., Wang, H.Q., Dupont, J.P., Rodet, J., Laignel, B. (2003). Assessment of direct transfer and resuspension of particles during turbid floods at a karstic spring. Journal of Hydrology, 275, 109-121 pp.

Masséi, N., Dupont, J.P., Mahler, B.J., Laignel, B., Fournier, M., Valdes, D., Ogier, S. (2006). Investigating transport properties and turbidity dynamics of a karst aquifer using correlation, spectral, and wavelet analyses. Journal of Hydrology, 329, 244-255 pp.

Merritt, W.S., Letcher, R.A., Jakeman, A.J. (2003). A review of erosion and sediment transport models. Environmental modelling & software, 18(8-9), 761-799 pp.

Meyers, G., Kapelan, Z., Keedwell, E., Randall-Smith, M. (2016). Short-term forecasting of turbidity in a UK water distribution system. Procedia Engineering, 154, 1140-1147 pp.

Meyers, G., Kapelan, Z., Keedwell, E. (2017). Short-term forecasting of turbidity in trunk main networks. Water research, 124, 67-76 pp.

Morgan, R.P.C. (2013). Soil Erosion and Conservation. https://doi.org/10.1002/9781118351475.ch22

Moriasi, D.N., Arnold, J.G., Van Liew, M.W., Bigner, R.L., Harmel, R.D., Veith, T.L. (2007). Model evaluation guidelines for systematic quantification of accuracy in watershed simulations. American Society of Agricultural and Biological Engineers, 50(3), 885-900 pp. ISSN 0001-2351

Nash, J.E. & Sutcliffe, J.V. (1970). River flow forecasting through conceptual models part I-a Discussion of Principles*. Journal of Hydrology, 10, 282-290 pp.

Ortiz-Rodriguez, J.M., Martinez-Blanco, M.R, Cervantes-Viramontes, J.M., Vega-Carrillo, H.R. (2013). Robust design of
555   artificial neural networks methodology in neutron spectrometry. In Artificial Neural Networks – Architectures and
Applications – Edition 1. Chapter 4, INTECH. https://dx.doi.org/10.5772/51274

Patault, E., Ledun, J., Landemaine, V., Soulignac, A., Richet, J-B., Ramaekers, F., Cikowski, N., Cabaz, B., Fournier, M.,
Ouvry, J-F., Rinaudo, J-D., Cerdan, O., Laignel, B. (2019). Coupled modeling of hydro-sedimentary transfer
processes and socio-economic dynamics evaluating public policies to control runoff and erosion: case study in
560   Normandy (France). AGU Fall Meeting 2019, San Francisco, USA. https://doi.org/10.1002/essoar.10501408.1

Patault, E., Ledun, J., Landemaine, V., Soulignac, A., Richet, J-B., Fournier, M., Rinaudo, J-D., Ouvry, J-F., Cerdan, O.,
Laignel, B. (2020). Evaluation de l'efficacité des politiques publiques pour les actions visant à réduire les impacts du
ruissellement et de l'érosion en Haute-Normandie. Rapport final. Université de Rouen Normandie – AREAS –
BRGM, 356 p.

565 Posthumus, H., Deeks, L.K., Rickson, R.J., Quinton, J.N. (2015). Costs and benefits of erosion control measures in the UK.
Soil Use and Management, 31, 16-33 pp. https://doi.org/10.1111/sum.12057

R Development Core Team (2008). R: A language and environment for statistical computing.R Foundation for Statistical
Computing, Vienna, Austria. ISBN 3-900051-07-0, URL http://www.R-project.org.

Renard, K.G & Freidmund J.R. (1994). Using monthly precipitation data to estimate the R factor in the revised USLE. Journal
570   of Hydrology, 157, 287-306 pp.

Ritters, A., Muñoz-Carpena, R. (2013). Performance evaluation of hydrological models: Statistical significance for reducing
subjectivity in goodness-of-fit assessments. Journal of Hydrology, 480, 33-45 pp.

Savary, M., Johannet, A., Masséi, N., Dupont, J-P., Hauchard, E. (2017). Operational turbidity forecast using both recurrent
and feed-forward based multilayer perceptrons. In: Rojas, I., Pomares, H., Valenzuela, O. (eds) Advances in time
575   series analysis and forecasting. ITISE 2016. Contributions to Statistics. Springer, Cham.

Shen, C. (2018). A transdisciplinary review of deep learning research and its relevance for water resources scientists. Water
Resources Research, 54, 8558-8593 pp. https://doi.org/10.1029/2018WR022643

Shen, C., Laloy, E., Elshorbagy, A., Albert, A., Bales, J., Chang, F-J., Ganguly, S., Hsu, K-L., Kifer, D., Fang, Z., Fang, K.,
Li, D., Li, X., Tsai, W-P. (2018). HESS Opinions: Incubating deep-learning-powered hydrologic science advances as
580   a community. Hydrol. Earth Syst. Sci., 22, 5639-5656 pp.

Siou, L.K.A., Johannet, A., Borrell, V., Pistre, S. (2011). Complexity selection of a neural network model for karst flood
forecasting: The case of the Lez Basin (southern France). Journal of Hydrology, 403, 367-380 pp.

Souchère, V., King, D., Daroussin, J., Papy, F., Capillon, A. (1998). Effects of tillage on runoff directions: Consequences on
runoff contributing area within agricultural catchments. J. Hydrol. 206, 256-267 pp. https://doi.org/10.1016/S0022-
585   1694(98)00103-6

Souchère, V., Cerdan, O., Ludwig, B., Le Bissonnais, Y., Couturier, A., Papy, F. (2003a). Modelling ephemeral gully erosion
in small cultivated catchments. Catena, 50, 489-505 pp. https://doi.org/10.1016/S0341-8162(02)00124-8

Souchère, V., Cerdan, O., Dubreuil, N., Le Bissonnais, Y., King, C. (2005). Modelling the impact of agri-environmental scenarios on runoff in a cultivated catchment (Normandy, France). Catena, 61, 229-240 pp.

590 Stevenson, M. & Bravo, C. (2019). Advanced turbidity prediction for operational water supply planning. Decision Support Systems, 119, 72-84 pp.

Takken, I., Beuselinck, L., Nachtergaele, J., Govers, G., Poesen, J., Degraer, G. Spatial Evaluation of physically-based distributed erosion model (LISEM). Catena, 37(3-4), 431-447 pp.

Varma, S., & Simon, R. (2006). Bias in error estimation when using cross-validation for model selection. BMC Bioinformatics, 595   7, 91; https://doi.org/10.1186/1471-2105-7-91

Vidal, J.P., Martin, E., Franchisteguy, L., Baillon, M. & Soubeyroux, J.M. (2010). A 50-year high-resolution atmospheric reanalysis over France with the Safran system. International Journal of Climatology, 30, 1627-1644 pp.

Wang, L. & Liu, H. (2006). An efficient method for identifying and filling surface depressions in digital elevation model for hydrologic analysis and modelling. Int. J. Geogr. Inf. Sci. 20, 193-213 pp. https://doi:10.1080/13658810500433453

600 Zhang, M.D.D., Yan, M.X.P., He, X. (2019). Modeling extreme events on time series prediction. KDD'19, august 4-8, 2019, anchorage, AK, USA. https://doi.org/10.1145/3292500.3330896